

ZEAL: Rethinking Large-Scale Resource Allocation with “Decouple and Decompose”

Zhiying Xu Francis Y. Yan Minlan Yu
Harvard University UIUC Harvard University

Abstract

Resource allocation is fundamental for cloud systems to ensure efficient resource sharing among tenants. However, the scale of such optimization problems has outgrown the capabilities of commercial solvers traditionally employed in production. To scale up resource allocation, prior approaches either tailor solutions to specific problems or rely on assumptions tied to particular workloads. In this work, we revisit real-world resource allocation problems and uncover a common underlying structure: a vast majority of these problems are inherently *separable*, i.e., they optimize the aggregate utility of individual resource and demand allocations, under separate constraints for each resource and each demand. Building on this insight, we develop ZEAL, a general, scalable, and theoretically grounded framework for accelerating resource allocation through a “decouple and decompose” approach. ZEAL systematically decouples entangled resource and demand constraints, thereby decomposing the overall optimization into alternating per-resource and per-demand allocations, which can then be solved efficiently and in parallel. We have implemented ZEAL as a library extension to an open-source solver, maintaining a familiar user interface. Experimental results across three prominent resource allocation tasks—traffic engineering, cluster scheduling, and load balancing—demonstrate ZEAL’s substantial speedups and robust allocation quality.

1 Introduction

Resource allocation is critical to the orchestration of multi-tenant systems, which are managed by today’s cloud providers on an unprecedented scale. It allows cloud services to be delivered with efficiency, reliability, and cost-effectiveness, by judiciously distributing various compute resources (e.g., CPUs and GPUs) and I/O resources (e.g., memory, storage, and network bandwidth) across a vast number of clients.

Common applications of resource allocation include cluster scheduling [27, 44, 46, 61, 64], traffic engineering [1, 24, 31, 50, 67], and load balancing [16, 37, 48, 52]. To meet varying user or application demands (jobs, traffic flows, and workloads), these systems extensively employ commercial optimization solvers like Gurobi [22] to compute the allocation of expensive cloud infrastructure (cluster resources, network links, and servers) worth millions or even billions of dollars.

As cloud environments rapidly expand and diversify, the sheer scale of modern resource allocation problems has ex-

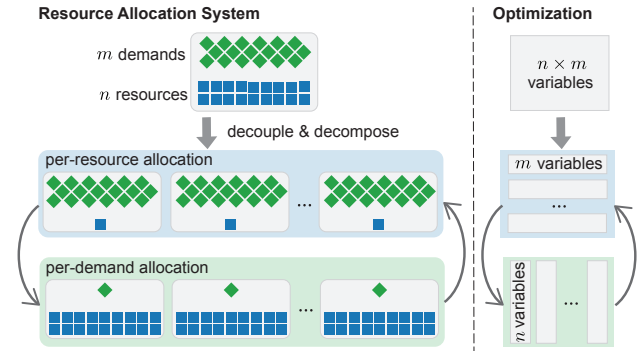


Figure 1: Overview of ZEAL.

ceeded the capabilities of commercial solvers. These problems may involve millions of variables, which require solvers tens of minutes to hours to compute a solution when fast allocation is needed to maintain service quality. This “scalability crisis” in resource allocation has prompted a flurry of recent research [1, 42, 43, 47, 63] that trades off allocation quality for speed using heuristics, approximate algorithms, or machine learning. Nevertheless, these studies are limited to either a single domain (e.g., wide-area network traffic engineering [1, 63]) or a specific objective (e.g., max-min fairness [42]), requiring substantial manual effort to adapt to new scenarios.

In contrast, POP [43] takes a general approach to accelerating assorted resource allocation problems. It partitions a large problem into a few (e.g., 16) subproblems, each with a subset of resources and demands, and solves them independently. However, this partition hinges on a “granular” assumption—each demand requests only a small fraction of mutually interchangeable resources. This assumption proves brittle with real workloads and degrades solution quality (§7.2).

In this study, we re-examine real-world resource allocation problems through a different lens and aim to develop a general and scalable optimization framework without catering to specific problems or making workload-dependent assumptions. Our approach, ZEAL, is theoretically grounded and enables fine-grained decomposition of the optimization problem, alternating between per-resource and per-demand allocations that can be solved in parallel (Figure 1).

This decomposition is made possible by an intrinsic, workload-agnostic problem structure that we uncovered after surveying dozens of real-world resource allocation problems in recent literature (Table 1). We discovered that a vast major-

ity of these problems are inherently *separable*: they optimize the sum (or maximum) of utilities (measurement of solution quality) from allocating each individual resource and demand, while ensuring feasible allocation for individual resource and demand as well.¹ In other words, the optimization objective comprises separate per-resource and/or per-demand utilities, and the constraints are also separate—they are either (1) a “resource constraint,” enforcing that the total demands mapped to each resource do not exceed the resource’s capacity, or (2) a “demand constraint,” enforcing that the total resources assigned to each demand do not surpass the demand’s needs. A formal definition of this separable structure is provided in §2, where we also show that real-world resource allocation is largely formulated with amenable mathematical properties (e.g., convex utilities, linear constraints) for tractability.²

Nonetheless, the uncovered “separability” in resource allocation problems does not directly allow us to actually separate them into independent subproblems that address individual resources and demands as depicted in Figure 1. This is because each resource not only appears in its own resource constraint but also participates in the demand constraints associated with every demand mapped to it; likewise for each demand. Ignoring the dependencies across subproblems and greedily solving each subproblem independently would fail to find feasible and high-quality allocations.

Given the intertwined nature of resource and demand constraints, ZEAL first *decouples* them as follows. Let x denote the resource allocation matrix between n resources and m demands, where x_{ij} represents the amount of resource i assigned to demand j . The key mathematical trick in ZEAL is to introduce a duplicate of the matrix x , denoted as z , along with an additional constraint $x = z$. Next, ZEAL iteratively and alternately solves for x subject only to resource constraints with z fixed, and solves for z subject only to demand constraints with x fixed. In each iteration, ZEAL further ensures that x and z do not deviate significantly from each other in order to satisfy $x = z$. This decoupling transformation lends itself to a classical constrained optimization framework called ADMM (Alternating Direction Method of Multipliers) [9]. ADMM allows ZEAL to embed each of the resource and demand constraints into the original objective as a penalty for constraint violation, thereby constructing augmented Lagrangians [23] as new optimization objectives. ADMM provides the theoretical foundation that enables alternating optimizations of these augmented Lagrangians with respect to x and z , respectively.

Next, ZEAL further *decomposes* the above optimizations into per-resource and per-demand allocations. This is feasible owing to the separable structure we identified across resource allocation problems: the original objective is separable on each resource and demand variable, and so are the penalty

terms converted by ADMM from constraints in the augmented Lagrangians. After decomposition, per-resource allocations involve solving n subproblems, each with m demand variables, and m subproblems with n resource variables for per-demand allocations. Consequently, the scale of optimization is greatly reduced from $n \times m$ variables to only n or m variables in each subproblem. These subproblems can be solved independently with massive parallelism using off-the-shelf solvers. Figure 2 illustrates the “decouple and decompose” workflow of ZEAL.

To demonstrate ZEAL’s practicality, we have implemented ZEAL as a Python package³, built on the widely used open-source solver `cvxpy` [4, 17]. The interface of ZEAL is also designed to resemble `cvxpy` for ease of use (§6). Moreover, instead of simulating the parallel execution of subproblems on multiple CPU cores as previous studies did [1, 43], we have carefully optimized ZEAL’s implementation using Ray [40], enabling efficient utilization of multiple cores without incurring significant overheads, such as cache contention.

We evaluate ZEAL in three prominent resource allocation problems—traffic engineering, cluster scheduling, and load balancing—and demonstrate its faster speed and higher allocation quality than the state of the art (§7). Compared with the best variant of POP [43] for each problem, ZEAL achieves a 5.3% higher allocation quality and a $7.6\times$ speedup in traffic engineering, 14% and $1.34\times$ in cluster scheduling, and 5.3% and $1.13\times$ in load balancing.

2 Real-World Resource Allocation Problems

In modern multi-tenant systems, resources such as CPUs, memory, and bandwidth are shared among numerous users and applications. A central resource allocator often casts the distribution of resources as an optimization problem (e.g., linear programming) and repeatedly computes feasible solutions with off-the-shelf solvers to accommodate changing demands.

However, these solvers are struggling to keep up with the increasing problem sizes that frequently occur in fast-growing systems. They may take *several hours* to solve an allocation problem that attempts to assign thousands of resources to thousands of demands—several orders of magnitude slower than desired (e.g., second-level SLAs, or service-level agreements). This challenge of scaling up resource allocation has spurred several recent works [1, 42, 43, 47, 63], but they either rely on domain-specific customizations or workload-dependent assumptions. In this paper, we instead seek to take a *general* (i.e., domain- and workload-agnostic) approach to scaling resource allocation.

After surveying real-world resource allocation problems from recent literature (Table 1), we discover that nearly all these formulations can be transformed into a *separable* structure (§1), which we formally describe as follows.

- *Variables.* An allocation matrix $x \in \mathcal{X}$ specifies how n resources should be shared among m demands, where x_{ij}

¹We focus on individually separable resources and demands for simplicity and due to their widespread presence in real systems, but they can be relaxed to *groups* of resources and demands as we show in §4.1.

²Rare exceptions to this common structure are discussed in §4.2.

³ZEAL can be installed with `pip install zeal` after publication.

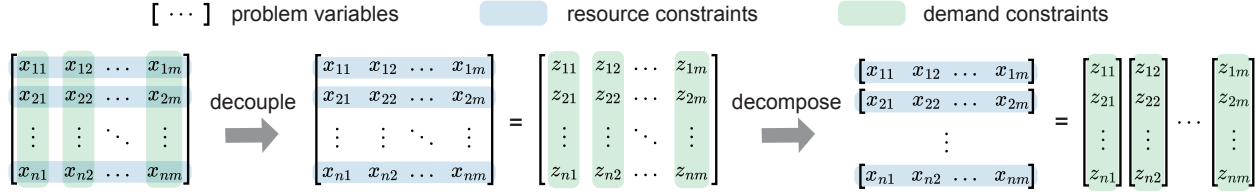


Figure 2: Workflow of ZEAL.

represents the quantity (or fraction) of resource i assigned to demand j . Accordingly, the i th row of x , denoted as $x_{i*} = [x_{i1}, x_{i2}, \dots, x_{im}]$, constitutes the allocation vector of resource i , and the j th column $x_{*j} = [x_{1j}, x_{2j}, \dots, x_{nj}]$ encodes the allocation of demand j . The constraint set \mathcal{X} is the Cartesian product of each \mathcal{X}_{ij} , which can be a set of real numbers or integers.

- *Objective.* The objective specifies a metric to be optimized over an allocation matrix x , primarily consisting of a sum of utilities (or costs, to measure allocation quality) from allocating each resource (x_{i*}) and demand (x_{*j}):

$$\sum_i f_i(x_{i*}) + \sum_j g_j(x_{*j}), \quad (1)$$

where $f_i(\cdot) : \mathbb{R}^m \rightarrow \mathbb{R}$ and $g_j(\cdot) : \mathbb{R}^n \rightarrow \mathbb{R}$ are utility (or cost) functions. They are typically designed to be convex to ensure practical tractability. Minimizing the maximum of utilities can also be converted into regular minimizing utilities (Equation 1) with additional constraints [5].

- *Constraints.* To ensure that individual resources and demands are not over-provisioned (i.e., exceeding a resource’s capacity or a demand’s requirements), there is typically a constraint for each resource and each demand. We observe that these constraints are largely linear, presumably for tractability as well. For simplicity, we further convert inequality constraints into equality constraints using non-negative slack variables (details in Section 6). As such, the resource constraint on resource i can be expressed as

$$R_i x_{i*} = r_i, \quad (2)$$

and the demand constraint on demand j can be written as

$$D_j x_{*j} = d_j. \quad (3)$$

Despite the separable objective and separable constraints over each resource and each demand, large resource allocation problems (e.g., with millions of variables) still remain painfully slow to solve as they cannot actually be “separated” into smaller, concurrent per-resource and per-demand subproblems. The main obstacle is that resource and demand constraints are fundamentally coupled. Equations 2 and 3 show that each $x_{i,j}$ not only participates in the resource constraint (over x_{i*}) but also in the demand constraint (over x_{*j}). Next, we describe our solution to this challenge.

3 ZEAL: Decouple and Decompose

We present ZEAL, a general, scalable, and theoretically rooted framework for optimizing real-world resource allocation problems. Leveraging the *separable* structure (§2) that underpins a vast majority of these problems, ZEAL enables massive parallelism with near-optimal solutions through a technique that we call “decouple and decompose.” A formal, mathematical representation of ZEAL is included in Appendix A.

3.1 Decouple

Resource and demand constraints being intertwined is the fundamental cause of complexity in resource allocation, as the individual allocation of any resource or demand will affect all other allocations. An optimal solution requires collectively allocating all resources to all demands, while a greedy strategy will lead to suboptimal or unfeasible solutions.

Existing domain-agnostic solutions do not address this intrinsic problem nature of resource allocation. Production systems employ commercial solvers and rely on linear programming (LP) or mixed-integer linear programming (MILP) algorithms (e.g., simplex methods [45], barrier methods [30], or branch-and-bound methods [8]) to iteratively explore the feasible region—a high-dimensional search space dictated by coupled resource and demand constraints.

The state of the art, POP [43], naively breaks intertwined constraints by partitioning resources and demands into a handful of subsets (e.g., 4–64), and then independently allocating each subset of resources to the demands within the same subset. Doing so ignores the dependencies across subsets and leads to suboptimal solutions in practice (§7.1). Meanwhile, it only enables limited parallelism because finer-grained decomposition would render the allocation unfeasible and unusable.

Instead of disregarding the constraints across subproblems, we tackle the intertwining root cause directly. Specifically, we aim to decouple demand constraints from resource constraints, transforming the full allocation into alternating *per-resource allocations*—assigning a resource to all demands subject to the corresponding resource constraint, and *per-demand allocations*—mapping a demand to all resources are subject to the corresponding demand constraint.

To begin with, we offload demand constraints to another variable different from x . We create a copy of the allocation matrix x , denoted as z , and replace the variables in each de-

mand constraint (Equation 3) with their counterparts in z :

$$D_{jz_*j} = d_j. \quad (4)$$

We also substitute z for the demand-related utilities in the objective function (Equation 1):

$$\sum_i f_i(x_{i*}) + \sum_j g_j(z_{*j}). \quad (5)$$

Then, representing the same allocation plan, x and z should be equal. Thus, we introduce a new constraint:

$$x = z. \quad (6)$$

Consequently, all resource constraints remain on x , but all demand constraints have been moved to z .

The decoupling of constraints clearly leads to a formulation equivalent to the original optimization with the new constraint $x = z$. However, the new constraint still has x and z entangled, so the introduction of z does not immediately enable decomposition. In fact, jointly optimizing x and z (e.g., using penalty methods [6] or the augmented Lagrangian method [23]) will forfeit the benefits of decoupling, as we will show in §7.3.

On the bright side, the transformed formulation becomes compatible with a half-century-old constrained optimization framework called ADMM (Alternating Direction Method of Multipliers) [9], which provides theoretically guaranteed solutions when solving for two sets (“blocks”) of variables (x and z). At a high level, the theory behind ADMM enables alternating optimization of the following subproblems without making compromises on the solution quality: minimizing the updated objective (Equation 5) with respect to

- x (with z fixed), subject to resource constraints and $x = z$,
- z (with x fixed), subject to demand constraints and $x = z$.

We elaborate in §3.2 that both optimization subproblems are amenable to decomposition, reducing problem sizes and enabling massive parallelism. Next, we first describe how ADMM solves them (even without decomposition).

- *Constraint transformation.* ADMM is a variant of the augmented Lagrangian method [23]. Taking the first subproblem above (for x) as an example: ADMM converts every constraint, i.e., resource constraints and $x = z$, into *penalty terms* and appends them to the objective to minimize (Equation 5). A conventional penalty method will add a single penalty term $\sum_i \mu \cdot c_i^2$ to the objective, where c_i is a measure of the constraint violation (comprising $|R_i x_{i*} - r_i|$ and $|x_i - z_i|$) for resource i , and μ is a penalty coefficient that increases to infinity over iterations to ensure asymptotic convergence to the optimal solution. However, taking μ to infinity requires careful manual tuning, or otherwise incurs ill-conditioning [2]. The augmented Lagrangian method has a similar rationale to penalty methods, except that it introduces yet another penalty term $\lambda_i \cdot c_i$ to mimic a Lagrange multiplier. The update of λ_i is automated as $\lambda_i \leftarrow \lambda_i + \mu \cdot c_i$

with theoretical guarantees, where μ can stay as a small constant while avoiding ill-conditioning.

- *Partial optimization.* The new objectives with additional penalty terms converted from constraint violations are also called *augmented Lagrangians*. ADMM alternately minimizes these augmented Lagrangians, solving for x with z fixed, and solving for z with x fixed. This is known as “two-block partial optimization” and guarantees the convergence to optimal solutions for convex problems [20, 21]. For non-convex problems (including those with integer variables), practical evidence suggests that ADMM is still effective at solving (some of) them as well [53, 62, 68]. Theoretical proofs are available under specific assumptions [38, 56, 60].

3.2 Decompose

To this point, the original resource allocation problem has been transformed into alternating minimization of two augmented Lagrangians (original objective plus penalty terms) with respect to x and z , respectively. Next, we take the x -minimization step as an example to describe how it can be decomposed (z -minimization is similar).

As x -minimization focuses on the variable x only, we can ignore terms related to z in the augmented Lagrangian, such as the penalty terms from demand constraints. The resulting objective consists of three resource-related terms:

- sum of per-resource allocation cost $f_i(x_{i*})$ from Equation 5;
- sum of penalties for violating each resource constraint $R_i x_{i*} = r_i$ from Equation 2;
- sum of penalties for violating $x = z$ from Equation 6.

The first two items are a sum of functions on per-resource allocation x_{i*} , while the third can also be rewritten as a sum of penalties for violating each $x_{i*} = z_{i*}$ (equivalent to $x = z$).

After rearranging, the optimization can be expressed as:

$$\min_{x \in \mathcal{X}} \sum_i F_i(x_{i*}),$$

where $F_i(x_{i*})$ consists of allocation cost, resource constraint penalty, and penalty for violating $x_{i*} = z_{i*}$. As each variable x_{i*} is mutually exclusive and independent, the above problem is equal to optimizing per-resource allocations in parallel:

$$\min_{x_{i*} \in \mathcal{X}_{i*}} F_i(x_{i*}), \quad \forall i,$$

thereby decomposing the allocation of x with $n \times m$ variables into n per-resource allocations of x_{i*} , each with m variables. To solve them, ZEAL uses an off-the-shelf solver (cvxpy in our implementation) to find (exact or approximate) solutions while making liberal use of all available CPU cores.

	Variables			Objective	
	Boolean	Integer	Float	Linear	Convex
RDC [55]	✓			✓	
SkyPilot [64]	✓				✓
ARROW [67], FlexWAN [39]	✓	✓		✓	
Shoofly [51]		✓	✓	✓	
PODP [7], RAS [46], Skyplane [26], Oort [34], TACCL [49], Shard Manager [37], Zeta [65], CASCARA [50], Sia [27], POP [43]	✓		✓	✓	
NetHint [14], Gavel [44], Teal [63], ONEWAN [32], BLASTSHIELD [31], NCFLOW [1], Cerebro [66], DOTE [47], Soroush [42], POP [43]			✓	✓	
PCF [29], Electricity Pricing [59], POP [43]			✓		✓

Table 1: Real-world resource allocation problems in recent literature.

4 Generality and Limitations

In this section, we start with the generality of ZEAL, and then discuss its limitations, including scenarios with limited parallelism and chances of suboptimal solutions.

4.1 Generality

ZEAL can be applied to a wide range of resource allocation problems. Table 1 presents a summary of real-world resource allocation problems in the recent literature, mostly from OSDI, SOSP, NSDI, and SIGCOMM in the past four years. Next, we explain why ZEAL is applicable.

- *Variables.* Inheriting from ADMM, ZEAL inherently supports real-number (float) allocation variables. Empirical evidence [53] and theoretical proofs [38, 56, 60] on ADMM also indicate that ZEAL can effectively handle boolean and integer variables by projecting real-number solutions to desired data types over iterations.
- *Objective.* ZEAL requires a max or sum of convex utility functions over per-resource or per-demand allocations. Most objectives used in systems exhibit convexity, such as the weighted allocation sum [44, 63], the logarithmic resource utility [3], and the quadratic allocation cost [59, 64].
- *Constraints.* ZEAL assumes the linearity of resource and demand constraints, which holds in all our surveyed problems, e.g., the sum of demands allocated to a resource must not exceed its capacity. The constraints in these problems are per resource or per demand as well. Even under a constraint on multiple resources or demands, ZEAL can be relaxed to groups of resources or demands. ZEAL bundles these groups together into per-resource-group or per-demand-group allocations during decomposition.

Unlike POP [43], ZEAL works with any workload, not only “granular” ones. In POP, the demands in each decomposed problem can access only a subset of resources, assuming each demand only requests a small fraction of interchangeable resources such that a resource subset suffices. This granular assumption can be unrealistic in practice, due to uneven

demand distributions [28, 57] or limited resources that each demand is allowed to utilize [33, 58]. In contrast, each decomposed problem in ZEAL can still access all the resources or demands; thus, the granular assumption is no longer required, affirming ZEAL’s generality to various workload types.

4.2 Limitations

While ZEAL applies to a variety of resource allocation problems, it might not always be the most suitable solution for every allocation problem.

Limited parallelism. ZEAL achieves parallelism by decomposing the full problem into per-resource and per-demand allocations. Therefore, when we cannot fully decompose the problem, ZEAL will experience limited parallelism, although this does not happen in our survey (Table 1).

- *Non-separable objectives.* When the objective function is not a sum or max over allocation qualities per resource or per demand, we must bundle per-resource or per-demand allocations whose utilities stick together during decomposition. As a result, the partially decomposed problem will achieve limited parallelism.
- *Non-separable constraints.* When a resource constraint restricts the allocation across multiple resources, we must bundle the allocations for these resources during decomposition, which leads to limited parallelism. This also applies to demand constraints.

Suboptimal solutions. It is possible for ZEAL not to attain an ideal solution when the allocation problem deviates from the standard ADMM formulation.

- *Non-convex problems.* ADMM can solve non-convex optimization problems [53, 62, 68] *empirically*, providing theoretical guarantees only under specific assumptions [38, 56, 60]. As a result, ZEAL can output suboptimal solutions in certain non-convex cases.
- *Nonlinear constraints.* When a constraint is nonlinear, we replace it by adding an indicator function to the objective. The indicator function is infinity when the constraint is

violated or otherwise zero. However, this may alter the convexity of the objective function, resulting in the above non-convex problems.

- *Higher allocation dimension.* The allocation of resources to demands is encoded in a two-dimensional matrix x . Correspondingly, we separate the problem into two ADMM blocks for resources and demands. Introducing more dimensions, such as a temporal dimension [36], leads to more ADMM blocks and risks convergence failure [13].

5 Case Studies

In this section, we will present case studies on how ZEAL can be applied to three resource allocation problems: traffic engineering, cluster scheduling, and load balancing, as also studied in POP [43].

5.1 Traffic Engineering

The traffic engineering problems [24, 42, 43, 54, 63] allocate traffic demand between datacenter nodes onto network links in a WAN topology.

Maximize total flow. The problem focuses on maximizing the total flow allocation.

- *Variables.* The flow allocation from datacenter node pair (s, t) onto network link (u, v) is denoted as $x_{(u,v)(s,t)} \geq 0$. In common path-based traffic engineering, flows between node pair (s, t) are allocated over links along pre-configured paths $P_{(s,t)}$ only.
- *Objective.* For a node pair (s, t) , the inflow it incurs to node v is computed as $\text{inflow}(v, (s, t)) = \sum_{(u,v) \in P_{s,t}} x_{(u,v)(s,t)}$ and outflow as $\text{outflow}(v, (s, t)) = \sum_{(v,u) \in P_{s,t}} x_{(v,u)(s,t)}$. The total flow allocated for the node pair (s, t) can be represented as $\text{inflow}(t, (s, t))$, which denotes the total inflow toward the destination t . Therefore, the objective of maximizing total flows between all node pairs can be expressed as the sum:

$$\text{Maximize}_x \sum_{(s,t)} \text{inflow}(t, (s, t)).$$

- *Resource constraints.* For each link (u, v) , the total flow allocation from all node pairs must not exceed its link capacity $c_{u,v}$:

$$\sum_{(s,t)} x_{(u,v)(s,t)} \leq c_{u,v}, \quad \forall (u, v) \in E.$$

- *Demand constraints.* For each node pair (s, t) , the total flow allocated cannot exceed the total demand. Additionally, for all nodes other than s and t , the inflow and outflow must be equal, ensuring no flow “black hole” along the paths:

$$\begin{aligned} 0 \leq \text{inflow}(t, (s, t)) &\leq d_{s,t}, \\ \text{inflow}(v, (s, t)) &= \text{outflow}(v, (s, t)), \forall v \neq s, t, \end{aligned} \quad \forall (s, t).$$

Min-max link utilization. The problem of min-max link utilization aims to allocate demands fairly over network links. The problem shares the same *variables* and linear *demand constraints* as the max total flow problem.

- *Objective.* The link utilization of a link (u, v) is the ratio between the total flow allocated on that link and link capacity. Our objective is to minimize the maximum utilization of each link:

$$\text{Minimize}_x \max_{(u,v) \in E} \frac{\sum_{(s,t)} x_{(u,v)(s,t)}}{c_{u,v}}.$$

Using ZEAL. The traffic engineering problem aligns the separable structure for ZEAL: the objectives are the sum of allocation quality per demand or the maximum of allocation quality per link, respectively. Linear constraints are applied to each demand and each link. Therefore, ZEAL can decompose the problem into $|E|$ per-link allocations and $|V|^2$ per-demand allocations for parallelism.

5.2 Cluster Scheduling

Cluster scheduling problems [42–44, 61] involves allocating jobs to computing resources (e.g., CPUs, GPUs) in heterogeneous clusters.

Max-min allocation. This problem aims to distribute the heterogeneous cluster resources fairly among jobs based on their effective throughput.

- *Variables.* With jobs time-sliced onto the available heterogeneous computing resources [43, 44], the allocation is a matrix $x \in [0, 1]^{n \times m}$ where x_{ij} is the fraction of time each job j spent on each computing resource type i .
- *Objective.* Given an allocation matrix x , we adopt a normalized effective throughput of job j from POP [41], which is a linear function on x_{*j} . The objective is to maximize the minimum allocation of normalized effective throughput:

$$\text{Maximize}_x \min_j \text{throughput}(j, x_{*j}).$$

- *Resource constraints.* For each computing resource type i , the total time allocation cannot exceed the number of that computing resource type:

$$\sum_j x_{ij} z_j \leq \text{num_workers}_i, \quad \forall i,$$

where z_j is the computing resources requested by job j .

- *Demand constraints.* For each job j , The sum of all fractions of time must be within 1:

$$\sum_i x_{ij} \leq 1, \quad \forall j.$$

Proportional fairness. The proportional fairness problem maximizes overall resource utilization while ensuring minimum service for each job. The problem shares the same *variables, resource constraints, and capacity constraints*.

- *Objective.* Proportional fairness aims to maximize the sum of log utilities of each job:

$$\text{Maximize}_x \sum_j \log(\text{throughput}(j, x_{*j})).$$

Using ZEAL. The cluster scheduling exhibits the separable structure required by ZEAL: The objective function is a minimum of allocation quality per job and a sum of allocation quality per job, respectively. Additionally, linear constraints are applied to each job and each computing resource. Thus, ZEAL can decompose the problem into n per-job allocations and m per-demand allocations.

5.3 Load Balancing

Load balancing problems [16, 43, 48, 52] allocate data shards among servers to scale out query loads in a distributed store.

Minimize shard movements. This problem aims to minimize shard movements across servers during load changes while keeping the load nearly balanced on each server.

- *Variables.* The allocation is a matrix $x \in [0, 1]^{n \times m}$, where x_{ij} is the fraction of data shard j allocated to server i . Additionally, a binary matrix x' captures shard placement, where $x'_{ij} = 1$ if the data shard j is on the server i , i.e., $x_{ij} > 0$; otherwise $x_{ij} = 0$.
- *Objective.* The movement of data shard j allocated to server i can be represent as $(1 - T_{ij})x'_{ij}f_j$, where T_{ij} denotes the initial shard placement and f_j denotes the memory footprint of data shard j . The objective of minimizing total shard movement can be expressed as the sum:

$$\text{Minimize}_x \sum_j \sum_i (1 - T_{ij})x'_{ij}f_j.$$

- *Resource constraints.* For each server i , the total query load must be close to the average query load L ; The total memory usage must be within memory capacity:

$$\begin{aligned} L - \epsilon &\leq \sum_j x_{ij}l_j \leq L + \epsilon, \\ \sum_j x'_{ij}f_j &\leq \text{memory}_i, \end{aligned} \quad \forall i,$$

where l_j is the query load on data shard j .

- *Demand constraints.* Each data shard j must allocate all the query load among servers:

$$\sum_i x_{ij} = 1, \quad \forall j.$$

Using ZEAL. Given the separable structure, where the objective is the sum of allocation quality per data shard and linear constraints apply to each server, and each shard, ZEAL can decompose the problem into n per-server allocations and m per-shard allocations.

```

1 import zeal
2
3 # Create allocation variables.
4 x = zeal.Variable((N, M), nonneg=True)
5
6 # Create the constraints.
7 resource_constrs = [
8     x[i,:].sum() <= 1 for i in range(N)]
9 demand_constrs = [
10    x[:,j].sum() <= 1 for j in range(M)]
11
12 # Create an objective.
13 obj = zeal.Minimize(x.sum())
14
15 # Construct and solve the problem.
16 prob = zeal.Problem(
17     obj, resource_constrs, demand_constrs)
18 prob.solve(num_cpus=64)

```

Listing 1: Resource allocation example with ZEAL package.

6 Implementation of ZEAL

We implement ZEAL as a Python package. After publication, we will upload ZEAL to PyPI for easy installation (`pip install zeal`).

Listing 1 showcases a simple resource allocation problem solved using our ZEAL package. In line 4, we initially create a $N \times M$ non-negative allocation variable x , where $x[i, j]$ represents the allocation of resource i to demand j . We then create a constraint for each resource in line 7–8 and a constraint for each demand in line 9–10, as well as an objective of minimizing the sum of x in line 13. Finally, we construct the problem in line 16–17 and solve it in line 18.

ZEAL borrows the interface from `cvxpy` [4, 17]. ZEAL inherits most of `cvxpy`'s methods, e.g. `Variable(.)` in line 4, `Minimize(.)` in line 13. One difference from `cvxpy` is that users must specify resource constraints and demands constraints separately (line 16–17) when initializing a problem. As a parallel solution, ZEAL allows users to specify the number of CPU cores (line 18); if not specified, ZEAL uses all available CPU cores.

Behind ZEAL's interface, the resource allocation problem is solved in the following three steps.

- *Problem parsing.* Inequality constraints are converted into equality constraints with a non-negative slack variable s , e.g., inequality `x[0, :].sum() <= 1` can be converted to equality `x[0, :].sum() + s == 1`. The slack variable can be regarded as an additional part of the problem variables and be optimized together.
- *Problem building.* Resource constraints are organized into independent per-resource subgroups without shared variables, while demand constraints are similarly organized into separate independent per-demand groups. For each subgroup, a per-resource or per-demand problem is built

using `cvxpy`, with the new objective formulated based on the augmented Lagrangian method outlined in § 3.2.

- *Problem solving.* Per-resource or per-demand problems in `cvxpy` are solved in parallel across multiple cores. Between ADMM iterations, only the parameters are updated, avoiding the need to rebuild the entire `cvxpy` problem. Similarly, for the same problem with varying resources and demands, only the corresponding parameters are updated.

We use Ray [40] to parallelize our computation across multiple cores. Python has limited parallelism in its multithreading implementation due to the notorious global interpreter lock (GIL). Instead, we choose Ray, which provides a wrapper for multiple Python interpreter processes, so as to avoid GIL. We also benefit from Ray’s production-grade implementation of inter-process coordination mechanisms to avoid building them from scratch using Python’s built-in low-level multiprocessing library.

7 Evaluation

We answer the following questions in the evaluation:

1. How does ZEAL compare with state-of-the-art approaches in allocation quality and computation time? (§7.1)
2. How do ZEAL and state-of-the-art approaches react to changes in problem granularity, temporal fluctuation, spatial redistribution, and link failures? (§7.2)
3. What is the contribution of each design in ZEAL? (§7.3)

We focus on four approaches throughout our evaluation:

- *Exact Sol.* Exact Sol solves the original resource allocation problem using commercial optimization solvers. We reuse the implementation from POP, which employs Gurobi [22], `cvxpy` [4, 17], and CPLEX [15] for traffic engineering, cluster engineering, and load balancing, respectively.
- *POP.* POP- k [43] randomly splits the problem into k smaller subproblems, applies commercial solvers in each, and coalesces the resulting k sub-allocations into a global allocation. However, POP only *simulates* the parallel execution by solving subproblems sequentially, collecting the solving time of each, and calculating the parallel solving time mathematically.
- *ZEAL.* ZEAL is our truly parallel implementation, with details described in Section 6.
- *ZEAL*.* To facilitate a fair comparison with POP, we create a variant of ZEAL, denoted as ZEAL*, following POP-style simulation where subproblems are solved sequentially and a parallel solving time is calculated mathematically.

We also consider domain-specific approaches apart from these four approaches. In traffic engineering, we evaluate a demand-pinning approach (“Pinning” for short) similar to a prior work [41], with the top 10% of demands allocated using optimization engines and the remaining assigned to the shortest paths. We also evaluate Teal [63], a learning-accelerated traffic engineering approach with massive paral-

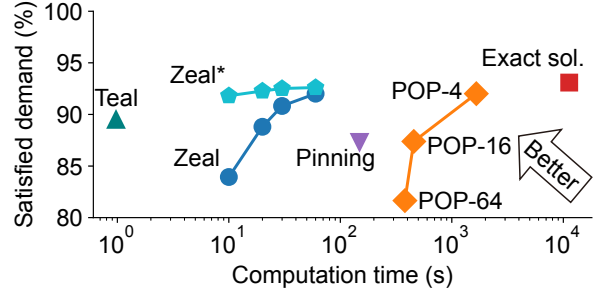


Figure 3: Comparison for the problem of maximizing total flow in traffic engineering.

lism achieved on the GPU. In cluster scheduling and load balancing, we evaluate the greedy heuristic algorithms, Gandiva [61] and E-Store [52], respectively.

We compare these approaches based on their allocation quality and computation times. The computation time is measured on 64 CPU cores (2× Intel Xeon Gold 6142); an additional GPU (Nvidia Titan RTX) is made available for Teal.

7.1 ZEAL vs. the State of the Art

In this section, we compare ZEAL against state-of-the-art approaches on resource allocation problems from Section 5.

7.1.1 Traffic Engineering

We adopt the largest network in Teal’s dataset for traffic engineering problems. This 1,739-node network is adapted from an AS-level internet topology [12] for WAN purposes, with the traffic data collected from a global cloud provider and then mapped into the large network.

Maximize total flow. Figure 3 compares ZEAL to state-of-the-art methods in maximizing total flow. ZEAL achieves 90.8% satisfied demand within 30 seconds and 92% within 60 seconds, demonstrating a superior trade-off between satisfied demand and computation time compared to Exact Sol, POP, and Pinning. While POP-4 also reaches 92% satisfied demand, its average computation time is significantly longer at 1658 seconds. POP-16 and POP-64 improve parallelism by dividing the workload into more subproblems, reducing computation times to 456 seconds and 380 seconds, respectively. Note that the speedup of POP-64 is limited compared to POP-16 as the number of cores per subproblem drops from 4 to 1. This increased parallelism also comes at a cost, with satisfied demand decreasing to 87.4% for POP-16 and 81.6% for POP-64. Pinning focuses on top demands to reduce problem size but remains constrained by the sequential nature of its optimization solvers. As a result, it achieves a modest speedup, requiring 149 seconds to reach 87.3% satisfied demand. Teal, a learning-accelerated approach, leverages massive GPU parallelism to achieve 89% satisfied demand in just 1 second. However, it relies on a highly customized machine-learning

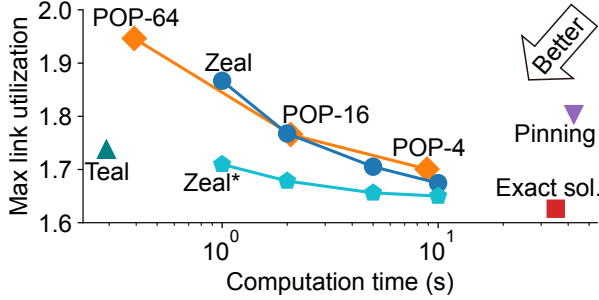


Figure 4: Comparison for the problem of minimizing max link utilization in traffic engineering.

framework, demanding significant human effort for design and training.

ZEAL*, representing the same algorithm under ideal conditions as POP, achieves a satisfied demand that is 8% higher than ZEAL within 10 seconds in Figure 3 and consistently delivers superior allocation quality across the other figures. The reason is that ZEAL* executes each iteration more quickly, allowing it to complete more iterations within a given time, resulting in higher allocation quality. The difference in iteration time between ZEAL and ZEAL* arises from three factors, as discussed in more detail in § 7.3: (1) ZEAL measures the end-to-end time, including problem-solving, compilation, solution unpacking, and other associated tasks, while ZEAL* only takes the problem-solving time into account. (2) ZEAL’s parallel implementation (§ 6) incurs overhead from cache contention, which slows down the problem-solving process. (3) In ZEAL, each subproblem is statically pre-assigned to one of the processes, making it susceptible to stragglers. In contrast, ZEAL* assumes perfect dynamic scheduling.

Min-max link utilization. Figure 4 compares ZEAL with other approaches in minimizing maximum link utilization. ZEAL achieves a low maximum link utilization of 1.67 within 10 seconds and 1.71 within 5 seconds. Exact Sol reaches 1.63 with an average computation time of 35 seconds, and it is faster than itself in maximizing total flow because minimizing max link utilization is "easier" and requires fewer iterations. Pinning takes 42.5 seconds, making it slower than ZEAL and slightly slower than Exact Sol, as it requires additional time to rebuild the problem when the top 10% of node pairs change. POP’s variants, POP-4, POP-16, and POP-64, achieve a maximum link utilization of 1.70, 1.77, and 1.95 with 9, 2, and 0.4 seconds on average, respectively. Although POP-16 is faster than ZEAL, a fairer comparison between POP-16 and ZEAL*, both simulating parallelism, reveals that ZEAL* achieves a comparable computation time to POP-16. The domain-specific solution Teal takes only 0.3 seconds with massive parallelism from GPU with a maximum link utilization of 1.74.

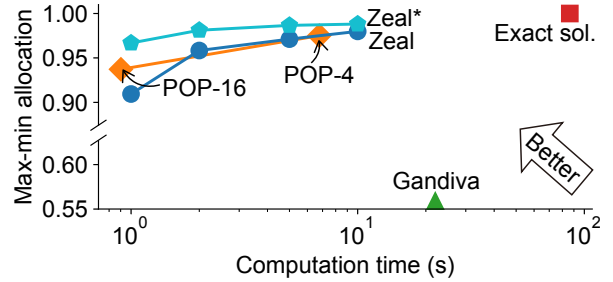


Figure 5: Comparison for the min-max allocation problem in cluster scheduling.

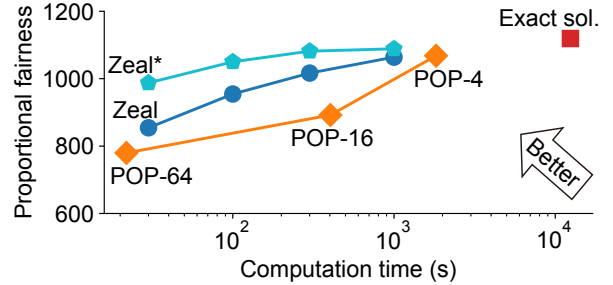


Figure 6: Comparison for the problem of maximizing proportional fairness in cluster scheduling.

7.1.2 Cluster Scheduling

We evaluate a large cluster scheduling problem of allocating jobs to 5000 GPU/CPU of 196 different types. We collect real throughput from two computing benchmarks [25, 35]. The number of GPU/CPU for each type and the required number in each job is generated based on the distribution observed in traces from real GPU-sharing clusters [58]. To reduce simulation time, we capture snapshots through the scheduling process rather than executing the entire simulation from start to finish.

Max-min allocation. Figure 5 compares ZEAL against other approaches with the objective of max-min allocation. ZEAL achieves a near-optimal max-min allocation of 0.97 within 5 seconds and 0.98 within 10 seconds, while ZEAL reaches 0.98 within 2 seconds. Due to their sequential nature, Exact Sol and Gandiva encounter a slow computation time of 86 and 22 seconds. The greedy heuristic Gandiva even experiences a 0.56 low max-min allocation. POP-4 delivers a comparable time-accuracy tradeoff as ZEAL but is 3.4× slower than ZEAL*, which is simulated in the same way as POP did for a fair comparison. A faster POP variant, POP-16, exhibits a lower max-min allocation of 0.94, as it becomes more difficult for jobs to assess the ideal GPU/CPU among the limited selection in smaller subproblems.

Proportional fairness. Figure 6 compares ZEAL against other approaches in maximizing proportional fairness. As the optimization problem becomes more difficult with the convex

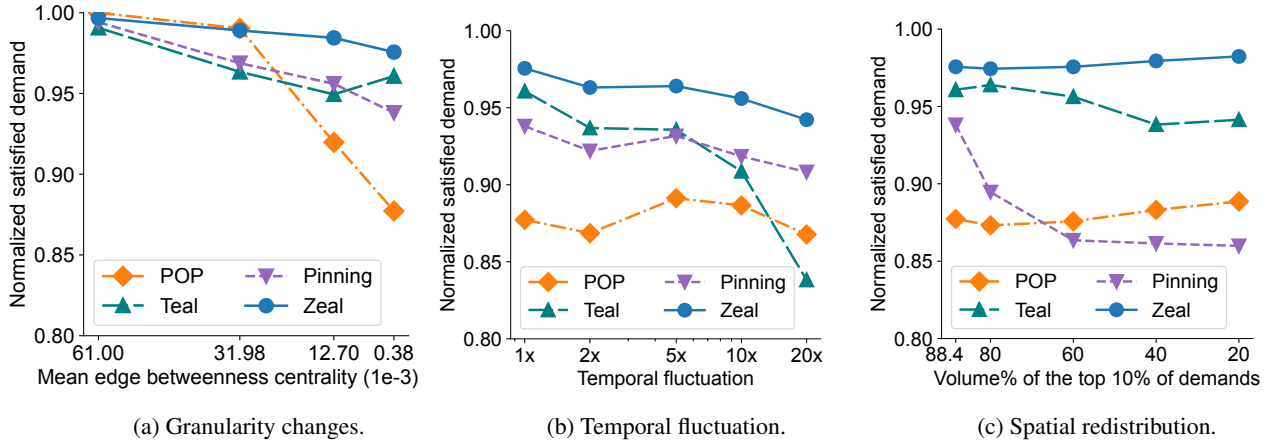


Figure 7: Normalized satisfied demand in traffic engineering against granularity, temporal, and spatial changes.

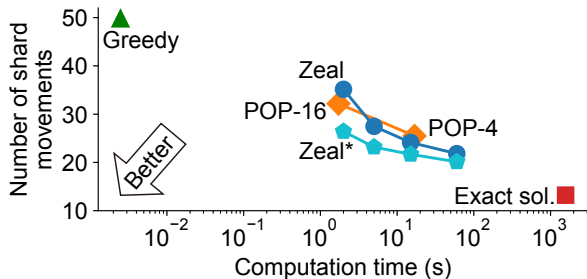


Figure 8: Comparison for the problem of minimizing shard movements in load balancing.

logarithm function in the objective, both ZEAL and ZEAL* achieve a greater speedup than POP by thoroughly breaking down the problem into smaller and easier pieces. ZEAL and ZEAL* reach a proportional fairness score of over 1,000 in 300 seconds and 100 seconds, respectively. In contrast, POP-4 takes 1,825 seconds to reach the same score, while POP-16 and POP-64 remain below 900 despite their shorter computation times. Exact Sol, though accurate, is prohibitively slow, requiring 12,432 seconds.

7.1.3 Load Balancing

We evaluate a load balancing problem of assigning 2048 data shards to 256 servers. In each round, we compute a new allocation of shards to servers given the new query loads [43].

Minimize shard movements. Figure 8 compares ZEAL with state-of-the-art approaches in minimizing shard movements. ZEAL achieves an average of 24.1 shard movements in 15 seconds, slightly better than POP-4’s 25.4 shard movements within 16.9 seconds. In faster scenarios, ZEAL achieves 35.1 shard movements in 2 seconds, while POP-4 achieves slightly fewer movements of 32.2 in 1.7 seconds. In a more fair comparison with POP, ZEAL* consistently costs 15–18% fewer shard movements than POP given a similar time limit. Exact Sol achieves the minimum shard movements of 13.2 but is

significantly slower, taking an average of 1,572 seconds due to the NP-hardness of solving the mixed-integer linear programming problem inherent to load balancing. On the other hand, the greedy heuristic represents the opposite end of the time-accuracy trade-off, completing in just 25 milliseconds but requiring 50 shard movements.

7.2 Robustness

We evaluate the robustness of ZEAL and other baselines against changes in problem granularity, temporal fluctuations, spatial redistribution, and link failures. In all these evaluations, ZEAL is run for 30 seconds. To mitigate the impact of the changing resources and demands, we normalize the satisfied demand by the optimal satisfied demand from Exact Sol.

Changes of problem granularity. The granular problem required by POP, where resources are mutually interchangeable, is impractical in reality. In traffic engineering, for example, demands are constrained to capacity resources on pre-configured paths. Similarly, in cluster scheduling, 33% of GPU tasks in production clusters are limited to specific GPU types [58]. Using traffic engineering as an example, we evaluate all approaches across varying levels of problem granularity, as depicted in Figure 7a. To quantify resource interchangeability, we use the mean edge betweenness centrality [10, 11], which measures the average percentage of demands served by a given edge.

As the mean edge betweenness centrality decreases, all approaches experience a decline in normalized satisfied demand, ranging from 0.8–2.1% for ZEAL, 2.8–4.2% for Teal, 2.5–5.6% for Pinning, and 1–12.3% for POP. However, the maximum decrease in POP is 5.9× greater than ZEAL because POP’s subproblems struggle to find alternative resources within their restricted subsets, whereas ZEAL’s subproblems retain access to the full set of resources. Teal exhibits a slight 1.3% increase in satisfied demand when the mean edge betweenness centrality is minimal. This is because the reduced edge selection simplifies allocation decisions.

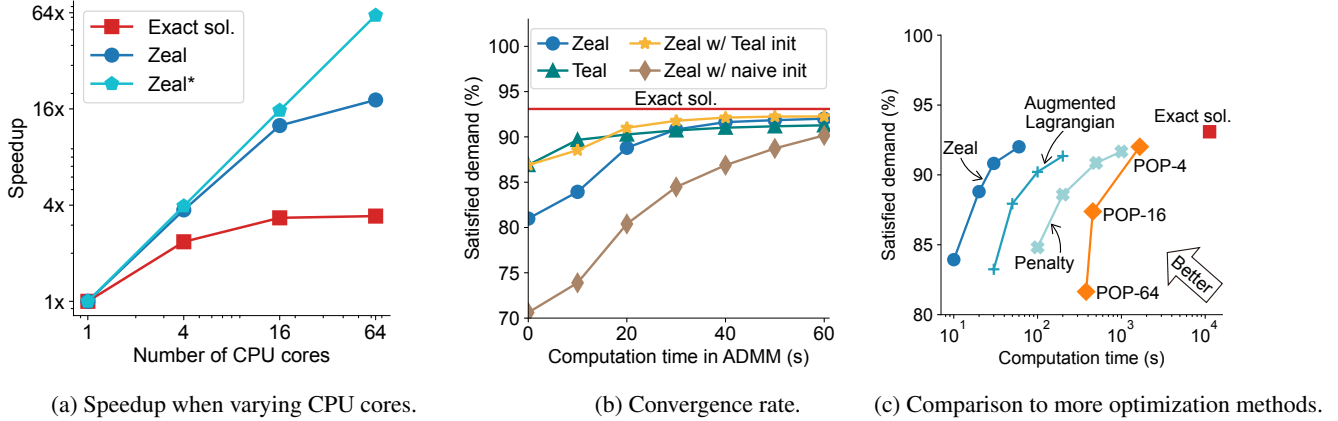


Figure 9: Micro-benchmarks with the objective of maximizing total flow in traffic engineering.

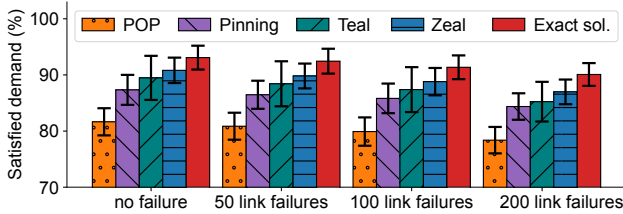


Figure 10: Satisfied demand of traffic engineering under zero, 50, 100, or 200 link failures after recomputing flow allocation.

Temporal fluctuation. We introduce temporal fluctuations [63] to the traffic matrices for robustness assessment. For each demand, we calculate the variance σ^2 in its changes between consecutive time slots and create a new normal distribution $N(0, k\sigma^2)$. We choose the values of k to be 2, 5, 10, and 20. Next, we randomly draw a sample from the newly created normal distribution and add it to each demand in every time slot, simulating temporal fluctuations.

Figure 7b demonstrates that ZEAL effectively manages temporal fluctuations, with changes in normalized satisfied demand limited to 1.3–3.5%. In contrast, Teal suffers a significant decrease of 12.8%, as it lacks prior exposure to the distribution of these fluctuating demands during training. Pinning and POP experience variations in normalized satisfied demand ranging from 0.6–3% and 1–1.6%, respectively. This is because randomness may occasionally favor splitting a problem into subproblems or focusing on top demands exclusively, while at other times, it does not.

Spatial redistribution. To evaluate robustness against spatial redistribution, we reassign traffic demands among node pairs. Specifically, we adjust the top 10% of demands, which initially account for 88.4% of the total volume, so that they take up 80%, 60%, 40%, and 20% of the total volume instead. Figure 7c shows that ZEAL consistently fulfills the highest demand across all spatial distributions. Pinning’s performance decreases by 8.3%, as its strategy of focusing only on top demands relies on the presence of a heavy-tailed dis-

tribution. Teal has a slight decrease up to 2.4% due to unseen demand distribution in training. This is a relatively smaller decrease than the temporal fluctuation, as Teal can still handle simple, evenly distributed traffic demands. POP has a slight increase of 1.4% as demands are more granular, where no demand requires a significant fraction of the total resources.

Link failures. In practice, large-scale inter-datacenter link failures are exceedingly rare. Even in the event of fiber link failures, they typically do not result in capacity loss on an inter-datacenter link, unless caused by a fiber cut [51]. As a stress test, however, we assess extreme failure scenarios described in previous work [67] and deliberately introduce 50, 100, and 200 link failures. Figure 10 illustrates the offline satisfied demand following these link failures, and we observe a consistent trend across different link failure scenarios across all approaches. Specifically, all approaches drop 0.6–1.1% under 50 link failures, 1.5–2.1% under 100 link failures, and 3–4.2% under 200 link failures. The reason is that these link failures constitute only a minor portion of the total 8,558 links, allowing all approaches to exhibit robustness given adequate time for re-computations.

7.3 Micro-benchmarks

We conduct micro-benchmarks to evaluate the impact of ZEAL’s design components, with all evaluations performed in maximizing total flow in traffic engineering.

Speedup when varying CPU cores. Figure 9a evaluates the speedup of ZEAL, ZEAL*, and Exact Sol with 1, 4, 16, and 64 CPU cores. ZEAL* achieves 61.7× speedup under 64 cores, where the slight gap occurs as we cannot exactly divide the total computation time evenly across 64 cores. ZEAL also achieves an almost linear speedup when the number of CPU cores grows from 1 to 16. However, this linearity diminishes with 64 cores, where ZEAL only achieves 18.2× speedup. This is because utilizing all 64 cores for parallelism incurs overhead from cache contention and stragglers, as discussed in Section 7.1. In contrast to the linear speedup of ZEAL* and

ZEAL, the speedup of Exact Sol is sublinear and marginal, achieving only $3.4\times$ speeds with 64 CPU cores. This is because of commercial solvers’ sequential nature, e.g., the simplex method [45] in linear programming requires thousands to millions of small steps to reach the optimal solution.

Convergence rate. Both Teal and ZEAL employ ADMM for parallel optimization, but their approaches differ. Teal’s ADMM adapts its computations based on matrix multiplication to leverage GPU calculation capabilities. Figure 9b illustrates the convergence rates of Teal and ZEAL under various initialization. ZEAL takes 30 seconds to surpass 90% satisfied demand. However, when initialized with Teal’s coarse neural network solution, ZEAL achieves this within 20 seconds. Conversely, with naive initialization, ZEAL requires more than 60 seconds. Teal, benefiting from the massive parallelism of GPUs, reaches 90% satisfied demand within 10 seconds. However, its adapted ADMM limits its performance, capping its satisfied demand at 91% at 60 seconds compared to ZEAL’s 92%.

Comparison to more optimization methods. Figure 9c investigates more constrained optimization methods other than ZEAL’s ADMM method in maximizing the total flow in traffic engineering. Section 7.1 has covered the computation time of the optimal Exact sol, the suboptimal POP-64, and the near-optimal ZEAL. As ZEAL replaces constraints with additional terms in the objective function, we compare similar methods, including the penalty method and the augmented Lagrangian method. The augmented Lagrangian method is the same as in ZEAL’s ADMM but without decoupling and decomposition, and thus it is over $3\times$ slower than ZEAL in reaching a satisfied demand of over 90%. The penalty method, which gradually increases penalty parameters from 0 to infinity to enforce the converted constraints in the objective function, converges slowly and is over $30\times$ slower than ZEAL in reaching a satisfied demand of over 90%.

8 Related Work

Resource allocation problems. Multi-tenant systems often address resource allocation challenges. Section 5 examines three prominent examples: cluster scheduling [27, 44, 46, 61, 64] allocates jobs to CPUs or GPUs in heterogeneous clusters, traffic engineering [1, 24, 31, 50, 67] allocates traffic demands to network link capacities in wide-area networks, and load balancing [16, 48, 52] allocates query loads to servers in distributed databases. Beyond these problems, Skyplane [26] allocates cloud resources (e.g., bandwidth and TCP connections) to overlay paths that traverse intermediate cloud regions, minimizing the cost of inter-region bulk transfers. Zeta [65] allocates traffic forwarding capability from gateway clusters to virtual private clouds for scalable and robust east-west communication in large-scale clouds. Shoofly [51] allocates light wavelengths of optical fiber to network shortcuts abstracted from optical bypasses, in order to minimize the hardware

costs of provisioning long-haul capacity.

Optimization algorithms. Various constrained optimization algorithms have been employed to solve resource allocation problems, depending on the variable types, objectives, and constraints. For linear programming problems like traffic engineering, the Gurobi solver [22] utilizes two primary methods. The simplex method [45] iteratively progresses along the boundaries of the feasible region toward the optimal solution, while the barrier method [30] iteratively approaches the optimal solution from within the feasible region. In mixed-integer linear programming like load balancing, the branch-and-bound method [8] divides the problem into smaller sub-problems, or branches, and then eliminates certain branches based on bounds on the optimal solution at each iteration. For more complex optimization problems, such as cone programming when maximizing proportional fairness in cluster scheduling, the ECOS algorithm [18] adopts a similar iterative process as the barrier methods, with search directions found by a symmetric indefinite KKT system. All these constrained optimization algorithms operate sequentially and iteratively, and thus introduce bottlenecks in solving time.

Decomposition for scalability. As resource allocation problems grow, efforts have been made to parallelize the iterative process in optimization algorithms for better scalability. NCFLOW [1] accelerates traffic engineering by partitioning the network into clusters and concurrently solving the flow allocation problem in each cluster. POP [43] targets “granular” allocation problems where resources are interchangeable. It randomly splits resources and demands into subsets and allocates each subset in parallel. Soroush [42] generalizes the classical waterfilling algorithm for max-min fair allocation and presents parallelizable combinatorial algorithms with fairness guarantees. Teal [63] models traffic engineering with neural networks to benefit from the massive parallelism in GPU. Eason et al. [19] employ the Benders decomposition algorithm to parallelize the design of a specialized cross-layer backbone network, offering performance guarantees for a particular allocation problem.

9 Conclusion

In this paper, we scale real-world resource allocation problems from a fresh perspective, observing that most of them exhibit an inherent *separable* structure. This key insight allows us to systematically decouple resource and demand constraints and decompose the original optimization problem into independent and parallel subproblems for allocating individual resources and demands. We implement this approach, ZEAL, as a library to augment a widely-used, open-source solver (cvxpy), offering a push-button solution that accelerates large-scale resource allocation. Through extensive evaluation across diverse resource allocation tasks, we demonstrate that ZEAL significantly improves scalability while closely approximating the quality of exact solutions.

References

- [1] Firas Abuzaid, Srikanth Kandula, Behnaz Arzani, Ishai Menache, Matei Zaharia, and Peter Bailis. Contracting Wide-area Network Topologies to Solve Flow Problems Quickly. In *18th USENIX Symposium on Networked Systems Design and Implementation (NSDI 21)*, pages 175–200, 2021.
- [2] Robert Acar and Curtis R. Vogel. Analysis of Bounded Variation Penalty Methods for Ill-posed Problems. *Inverse problems*, 10(6):1217, 1994.
- [3] Akshay Agrawal, Stephen Boyd, Deepak Narayanan, Fiodar Kazhamiaka, and Matei Zaharia. Allocation of Fungible Resources via a Fast, Scalable Price Discovery Method. *Mathematical Programming Computation*, 14(3):593–622, 2022.
- [4] Akshay Agrawal, Robin Verschueren, Steven Diamond, and Stephen Boyd. A rewriting system for convex optimization problems. *Journal of Control and Decision*, 5(1):42–60, 2018.
- [5] Ravindra K. Ahuja. Minimax Linear Programming Problem. *Operations Research Letters*, 4(3):131–134, 1985.
- [6] Achim Bachem, Martin Grötschel, and Bernhard Korte. Mathematical Programming the State of the Art: Bonn 1982. 2012.
- [7] Nirvik Baruah, Peter Kraft, Fiodar Kazhamiaka, Peter Bailis, and Matei Zaharia. Parallelism-Optimizing Data Placement for Faster Data-Parallel Computations. *Proceedings of the VLDB Endowment*, 16(4):760–771, 2022.
- [8] Stephen Boyd and Jacob Mattingley. Branch and bound methods. *Notes for EE364b, Stanford University*, 2006:07, 2007.
- [9] Stephen Boyd, Neal Parikh, Eric Chu, Borja Peleato, Jonathan Eckstein, et al. Distributed Optimization and Statistical Learning via the Alternating Direction Method of Multipliers. *Foundations and Trends in Machine Learning*, 3(1):1–122, 2011.
- [10] Ulrik Brandes. A Faster Algorithm for Betweenness Centrality. *Journal of mathematical sociology*, 25(2):163–177, 2001.
- [11] Ulrik Brandes. On variants of shortest-path betweenness centrality and their generic computation. *Social networks*, 30(2):136–145, 2008.
- [12] CAIDA. The CAIDA AS Relationships Dataset, 2024.
- [13] Caihua Chen, Bingsheng He, Yinyu Ye, and Xiaoming Yuan. The Direct Extension of ADMM for Multi-block Convex Minimization Problems is Not Necessarily Convergent. *Mathematical Programming*, 155(1):57–79, 2016.
- [14] Jingrong Chen, Hong Zhang, Wei Zhang, Liang Luo, Jeffrey Chase, Ion Stoica, and Danyang Zhuo. NetHint: White-Box Networking for Multi-Tenant Data Centers. In *19th USENIX Symposium on Networked Systems Design and Implementation (NSDI 22)*, pages 1327–1343, 2022.
- [15] IBM ILOG Cplex. V12. 1: User’s Manual for CPLEX. *International Business Machines Corporation*, 46(53):157, 2009.
- [16] Carlo Curino, Evan PC Jones, Samuel Madden, and Hari Balakrishnan. Workload-aware Database Monitoring and Consolidation. In *Proceedings of the 2011 ACM SIGMOD International Conference on Management of data*, pages 313–324, 2011.
- [17] Steven Diamond and Stephen Boyd. CVXPY: A Python-embedded modeling language for convex optimization. *Journal of Machine Learning Research*, 17(83):1–5, 2016.
- [18] Alexander Domahidi, Eric Chu, and Stephen Boyd. ECOS: An SOCP solver for embedded systems. In *2013 European control conference (ECC)*, pages 3071–3076. IEEE, 2013.
- [19] John P. Eason, Xueqi He, Richard Cziva, Max Noormohammadpour, Srivatsan Balasubramanian, Satyajeet Singh Ahuja, and Biao Lu. Hose-based Cross-layer Backbone Network Design with Benders Decomposition. In *Proceedings of the ACM SIGCOMM 2023 Conference*, pages 333–345, 2023.
- [20] Daniel Gabay and Bertrand Mercier. A Dual Algorithm for the Solution of Nonlinear Variational Problems via Finite Element Approximation. *Computers & mathematics with applications*, 2(1):17–40, 1976.
- [21] Roland Glowinski and Americo Marroco. Sur l’approximation, par éléments finis d’ordre un, et la résolution, par pénalisation-dualité d’une classe de problèmes de Dirichlet non linéaires. *Revue française d’automatique, informatique, recherche opérationnelle. Analyse numérique*, 9(R2):41–76, 1975.
- [22] Gurobi Optimization, LLC. Gurobi Optimizer Reference Manual, 2023.
- [23] Magnus R. Hestenes. Multiplier and Gradient Methods. *Journal of optimization theory and applications*, 4(5):303–320, 1969.
- [24] Chi-Yao Hong, Srikanth Kandula, Ratul Mahajan, Ming Zhang, Vijay Gill, Mohan Nanduri, and Roger Wattenhofer. Achieving High Utilization with Software-driven WAN. In *Proceedings of the ACM SIGCOMM 2013 Conference on SIGCOMM*, pages 15–26, 2013.
- [25] Andrey Ignatov, Radu Timofte, Andrei Kulik, Seungsoo Yang, Ke Wang, Felix Baum, Max Wu, Lirong Xu, and Luc Van Gool. AI Benchmark: All about Deep Learning on Smartphones in 2019. In *2019 IEEE/CVF International Conference on Computer Vision Workshop (ICCVW)*, pages 3617–3635. IEEE, 2019.
- [26] Paras Jain, Sam Kumar, Sarah Wooders, Shishir G. Patil, Joseph E. Gonzalez, and Ion Stoica. Skyplane: Optimizing Transfer Cost and Throughput Using Cloud-Aware Overlays. In *20th USENIX Symposium on Networked Systems Design and Implementation*, pages 1375–1389, 2023.
- [27] Suhas Jayaram Subramanya, Daiyaan Arfeen, Shouxu Lin, Aurick Qiao, Zhihao Jia, and Gregory R. Ganger. Sia: Heterogeneity-aware, goodput-optimized ML-cluster scheduling. In *Proceedings of the 29th Symposium on Operating Systems Principles*, pages 642–657, 2023.
- [28] Myeongjae Jeon, Shivaram Venkataraman, Amar Phanishayee, Junjie Qian, Wencong Xiao, and Fan Yang. Analysis of Large-Scale Multi-Tenant GPU clusters for DNN training workloads. In *2019 USENIX Annual Technical Conference (USENIX ATC 19)*, pages 947–960, 2019.
- [29] Chuan Jiang, Sanjay Rao, and Mohit Tawarmalani. PCF: Provably Resilient Flexible Routing. In *Proceedings of the Annual conference of the ACM Special Interest Group on Data Communication on the applications, technologies, architectures, and protocols for computer communication*, pages 139–153, 2020.
- [30] Narendra Karmarkar. A New Polynomial-time Algorithm for Linear Programming. In *Proceedings of the sixteenth annual ACM symposium on Theory of computing*, pages 302–311, 1984.
- [31] Umesh Krishnaswamy, Rachee Singh, Nikolaj Bjørner, and Himanshu Raj. Decentralized cloud wide-area network traffic engineering with BlastShield. In *19th USENIX Symposium on Networked Systems Design and Implementation (NSDI 22)*, pages 325–338, 2022.
- [32] Umesh Krishnaswamy, Rachee Singh, Paul Mattes, Paul-Andre C. Bissonnette, Nikolaj Bjørner, Zahira Nasrin, Sonal Kothari, Prabhakar Reddy, John Abeln, Srikanth Kandula, et al. OneWAN is better than two: Unifying a split WAN architecture. In *20th USENIX Symposium on Networked Systems Design and Implementation (NSDI 23)*, pages 515–529, 2023.
- [33] Praveen Kumar, Yang Yuan, Chris Yu, Nate Foster, Robert Kleinberg, Petr Lapukhov, Chiun Lin Lim, and Robert Soulé. Semi-oblivious Traffic Engineering: The Road not Taken. In *15th USENIX Symposium on Networked Systems Design and Implementation (NSDI 18)*, pages 157–170, 2018.
- [34] Fan Lai, Xiangfeng Zhu, Harsha V. Madhyastha, and Mosharaf Chowdhury. Oort: Efficient federated learning via guided participant selection. In *15th USENIX Symposium on Operating Systems Design and Implementation*, pages 19–35, 2021.
- [35] Lambda. Deep Learning GPU Benchmarks, 2024.

- [36] Tan N. Le, Xiao Sun, Mosharaf Chowdhury, and Zhenhua Liu. Allox: Compute Allocation in Hybrid Clusters. In *Proceedings of the Fifteenth European Conference on Computer Systems*, pages 1–16, 2020.
- [37] Sangmin Lee, Zhenhua Guo, Omer Sunercan, Jun Ying, Thawan Kooburat, Suryadeep Biswal, Jun Chen, Kun Huang, Yatpang Cheung, Yiding Zhou, et al. Shard Manager: A Generic Shard Management Framework for Geo-distributed Applications. In *Proceedings of the ACM SIGOPS 28th Symposium on Operating Systems Principles*, pages 553–569, 2021.
- [38] Sleiman Mhanna, Gregor Verbič, and Archie C. Chapman. Adaptive ADMM for Distributed AC Optimal Power Flow. *IEEE Transactions on Power Systems*, 34(3):2025–2035, 2018.
- [39] Congcong Miao, Zhizhen Zhong, Ying Zhang, Kunling He, Fangchao Li, Minggang Chen, Yiren Zhao, Xiang Li, Zekun He, Xianneng Zou, et al. FlexWAN: Software Hardware Co-design for Cost-Effective and Resilient Optical Backbones. In *Proceedings of the ACM SIGCOMM 2023 Conference*, pages 319–332, 2023.
- [40] Philipp Moritz, Robert Nishihara, Stephanie Wang, Alexey Tumanov, Richard Liaw, Eric Liang, Melih Elibol, Zongheng Yang, William Paul, Michael I. Jordan, et al. Ray: A Distributed Framework for Emerging AI Applications. In *13th USENIX symposium on operating systems design and implementation (OSDI 18)*, pages 561–577, 2018.
- [41] Pooria Namyar, Behnaz Arzani, Ryan Beckett, Santiago Segarra, Himanshu Raj, and Srikanth Kandula. Minding the Gap between Fast Heuristics and their Optimal Counterparts. In *Proceedings of the 21st ACM Workshop on Hot Topics in Networks*, pages 138–144, 2022.
- [42] Pooria Namyar, Behnaz Arzani, Srikanth Kandula, Santiago Segarra, Daniel Crankshaw, Umesh Krishnaswamy, Ramesh Govindan, and Himanshu Raj. Solving Max-Min Fair Resource Allocations Quickly on Large Graphs. In *21th USENIX Symposium on Networked Systems Design and Implementation (NSDI 24)*, 2024.
- [43] Deepak Narayanan, Fiodar Kazhamiaka, Firas Abuzaid, Peter Kraft, Akshay Agrawal, Srikanth Kandula, Stephen Boyd, and Matei Zaharia. Solving Large-Scale Granular Resource Allocation Problems Efficiently with POP. In *Proceedings of the ACM SIGOPS 28th Symposium on Operating Systems Principles*, pages 521–537, 2021.
- [44] Deepak Narayanan, Keshav Santhanam, Fiodar Kazhamiaka, Amar Phanishayee, and Matei Zaharia. Heterogeneity-Aware Cluster Scheduling Policies for Deep Learning Workloads. In *14th USENIX Symposium on Operating Systems Design and Implementation*, pages 481–498, 2020.
- [45] John A. Nelder and Roger Mead. A Simplex Method for Function Minimization. *The computer journal*, 7(4):308–313, 1965.
- [46] Andrew Newell, Dimitrios Skarlatos, Jingyuan Fan, Pavan Kumar, Maxim Khutornenko, Mayank Pundir, Yirui Zhang, Mingjun Zhang, Yuanlai Liu, Linh Le, et al. RAS: Continuously Optimized Region-Wide Datacenter Resource Allocation. In *Proceedings of the ACM SIGOPS 28th Symposium on Operating Systems Principles*, pages 505–520, 2021.
- [47] Yarin Perry, Felipe Vieira Frujeri, Chaim Hoch, Srikanth Kandula, Ishai Menache, Michael Schapira, and Aviv Tamar. DOTE: Rethinking (Predictive) WAN Traffic Engineering. In *20th USENIX Symposium on Networked Systems Design and Implementation (NSDI 23)*, pages 1557–1581, 2023.
- [48] Marco Serafini, Essam Mansour, Ashraf Aboulmaga, Kenneth Salem, Taha Rafiq, and Umar Farooq Minhas. Accordion: Elastic Scalability for Database Systems Supporting Distributed Transactions. *Proceedings of the VLDB Endowment*, 7(12):1035–1046, 2014.
- [49] Aashaka Shah, Vijay Chidambaram, Meghan Cowan, Saeed Maleki, Madan Musuvathi, Todd Mytkowicz, Jacob Nelson, Olli Saarikivi, and Rachee Singh. TACCL: Guiding Collective Algorithm Synthesis using Communication Sketches. In *20th USENIX Symposium on Networked Systems Design and Implementation*, pages 593–612, 2023.
- [50] Rachee Singh, Sharad Agarwal, Matt Calder, and Paramvir Bahl. Cost-effective Cloud Edge Traffic Engineering with CASCARA. In *18th USENIX Symposium on Networked Systems Design and Implementation (NSDI 21)*, pages 201–216, 2021.
- [51] Rachee Singh, Nikolaj Björner, Sharon Shoham, Yawei Yin, John Arnold, and Jamie Gaudette. Cost-effective Capacity Provisioning in Wide Area Networks with Shoofly. In *Proceedings of the 2021 ACM SIGCOMM 2021 Conference*, pages 534–546, 2021.
- [52] Rebecca Taft, Essam Mansour, Marco Serafini, Jennie Duggan, Aaron J. Elmore, Ashraf Aboulmaga, Andrew Pavlo, and Michael Stonebraker. E-store: Fine-grained Elastic Partitioning for Distributed Transaction Processing Systems. *Proceedings of the VLDB Endowment*, 8(3):245–256, 2014.
- [53] Reza Takapoui, Nicholas Moehle, Stephen Boyd, and Alberto Bemporad. A Simple Effective Heuristic for Embedded Mixed-integer Quadratic Programming. *International journal of control*, 93(1):2–12, 2020.
- [54] Asaf Valadarsky, Michael Schapira, Dafna Shahaf, and Aviv Tamar. Learning to Route. In *Proceedings of the 16th ACM workshop on hot topics in networks*, pages 185–191, 2017.
- [55] Weitao Wang, Dingming Wu, Sushovan Das, Afsaneh Rahbar, Ang Chen, and TS Eugene Ng. RDC: Energy-Efficient Data Center Network Congestion Relief with Topological Reconfigurability at the Edge. In *19th USENIX Symposium on Networked Systems Design and Implementation*, pages 1267–1288, 2022.
- [56] Yu Wang, Wotao Yin, and Jinshan Zeng. Global Convergence of ADMM in Nonconvex Nonsmooth Optimization. *Journal of Scientific Computing*, 78:29–63, 2019.
- [57] Zhaohua Wang, Zhenyu Li, Guangming Liu, Yunfei Chen, Qinghua Wu, and Gang Cheng. Examination of WAN Traffic Characteristics in a Large-scale Data Center Network. In *Proceedings of the 21st ACM Internet Measurement Conference*, pages 1–14, 2021.
- [58] Qizhen Weng, Lingyun Yang, Yinghao Yu, Wei Wang, Xiaochuan Tang, Guodong Yang, and Liping Zhang. Beware of Fragmentation: Scheduling GPU-Sharing Workloads with Fragmentation Gradient Descent. In *2023 USENIX Annual Technical Conference, USENIX ATC '23*. USENIX Association, 2023.
- [59] Lucien Werner, Adam Wierman, and Steven H. Low. Pricing Flexibility of Shiftable Demand in Electricity Markets. In *Proceedings of the Twelfth ACM International Conference on Future Energy Systems*, pages 1–14, 2021.
- [60] Baoyuan Wu and Bernard Ghanem. l_p -Box ADMM: A Versatile Framework for Integer Programming. *IEEE transactions on pattern analysis and machine intelligence*, 41(7):1695–1708, 2018.
- [61] Wencong Xiao, Romil Bhardwaj, Ramachandran Ramjee, Muthian Sivathanu, Nipun Kwatra, Zhenhua Han, Pratyush Patel, Xuan Peng, Hanyu Zhao, Quanlu Zhang, et al. Gandiva: Introspective Cluster Scheduling for Deep Learning. In *13th USENIX Symposium on Operating Systems Design and Implementation (OSDI 18)*, pages 595–610, 2018.
- [62] Zheng Xu, Soham De, Mario Figueiredo, Christoph Studer, and Tom Goldstein. An Empirical Study of ADMM for Nonconvex Problems. *arXiv preprint arXiv:1612.03349*, 2016.
- [63] Zhiying Xu, Francis Y. Yan, Rachee Singh, Justin T. Chiu, Alexander M. Rush, and Minlan Yu. Teal: Learning-Accelerated Optimization of WAN Traffic Engineering. In *Proceedings of the ACM SIGCOMM 2023 Conference*, pages 378–393, 2023.
- [64] Zongheng Yang, Zhanghao Wu, Michael Luo, Wei-Lin Chiang, Romil Bhardwaj, Woosuk Kwon, Siyuan Zhuang, Frank Sifei Luan, Gautam Mittal, Scott Shenker, et al. SkyPilot: An Intercloud Broker for Sky Computing. In *20th USENIX Symposium on Networked Systems Design and Implementation*, pages 437–455, 2023.

- [65] Qianyu Zhang, Gongming Zhao, Hongli Xu, Zhuolong Yu, Liguang Xie, Yangming Zhao, Chunming Qiao, Ying Xiong, and Liusheng Huang. Zeta: A Scalable and Robust East-West Communication Framework in Large-Scale Clouds. In *19th USENIX Symposium on Networked Systems Design and Implementation*, pages 1231–1248, 2022.
- [66] Wenting Zheng, Ryan Deng, Weikeng Chen, Raluca Ada Popa, Aurojit Panda, and Ion Stoica. Cerebro: A Platform for Multi-Party Cryptographic Collaborative Learning. In *30th USENIX Security Symposium (USENIX Security 21)*, pages 2723–2740, 2021.
- [67] Zhizhen Zhong, Manya Ghobadi, Alaa Khaddaj, Jonathan Leach, Yiting Xia, and Ying Zhang. ARROW: Restoration-Aware Traffic Engineering. In *Proceedings of the 2021 ACM SIGCOMM 2021 Conference*, pages 560–579, 2021.
- [68] Jun Zhou, Yang Bao, Daohong Jian, and Hua Wu. PDAS: A Practical Distributed ADMM System for Large-Scale Linear Programming Problems at Alipay. In *Proceedings of the 29th ACM SIGKDD Conference on Knowledge Discovery and Data Mining*, pages 5717–5727, 2023.

A Mathematical Representation of ZEAL

A resource allocation problem can be written as

$$\min_{x \in \mathcal{X}} \sum_i f_i(x_{i*}) + \sum_j g_j(x_{*j}), \quad (1)$$

$$s.t. \quad R_i x_{i*} = r_i, \quad \forall i, \quad (2)$$

$$D_j x_{*j} = d_j, \quad \forall j, \quad (3)$$

where Equation 1 is the objective, and Equation 2 and Equation 3 are resource constraints and demand constraints, respectively.

Our first step decouples resource and demand constraints. We create a copy of the allocation variable x , denoted as z , and replace the variable x in demand constraints (Equation 3) as well as the demand-related portion of the objective function (Equation 1) with the variable z . We also add a new constraint $x = z$ (Equation 6) to keep x and z equal.

$$\min_{x \in \mathcal{X}} \sum_i f_i(x_{i*}) + \sum_j g_j(z_{*j}), \quad (1)$$

$$s.t. \quad R_i x_{i*} = r_i, \quad \forall i, \quad (2)$$

$$D_j z_{*j} = d_j, \quad \forall j, \quad (3)$$

$$x - z = 0. \quad (6)$$

We rewrite our problem in the Augmented Lagrangian to move the constraints to the objective function:

$$\begin{aligned} \mathcal{L}_p(x, z, \alpha, \beta, \lambda) &= \sum_i f_i(x_{i*}) + \sum_j g_j(z_{*j}) \\ &+ \frac{\rho}{2} \left(\sum_i \|R_i x_{i*} - r_i + \alpha_i\|_2^2 + \sum_j \|D_j z_{*j} - d_j + \beta_j\|_2^2 \right) \\ &+ \|x - z + \lambda\|_F^2 - \frac{\rho}{2} (\|\alpha\|_2^2 + \|\beta\|_2^2 + \|\lambda\|_F^2). \end{aligned}$$

ADMM allows partial optimization alternatively on x and

z :

$$x^{(k+1)} := \arg \min_{x \in \mathcal{X}} \mathcal{L}_p(x, z^{(k)}, \alpha^{(k)}, \beta^{(k)}, \lambda^{(k)}) \quad (7)$$

$$z^{(k+1)} := \arg \min_z \mathcal{L}_p(x^{(k+1)}, z, \alpha^{(k)}, \beta^{(k)}, \lambda^{(k)}) \quad (8)$$

$$\alpha_i^{(k+1)} := \alpha_i^{(k)} + R_i x_{i*}^{(k+1)} - r_i, \forall i$$

$$\beta_j^{(k+1)} := \beta_j^{(k)} + D_j z_{*j}^{(k+1)} - d_j, \forall j$$

$$\lambda^{(k+1)} := \lambda^{(k)} + x^{(k+1)} - z^{(k+1)}$$

Our second step further decomposes the partial optimization into optimizing each row in x and each column in z . We rewrite Equation 7 as

$$\begin{aligned} x^{(k+1)} &= \arg \min_{x \in \mathcal{X}} \mathcal{L}_p(x, z^{(k)}, \alpha^{(k)}, \beta^{(k)}, \lambda^{(k)}) \quad (7) \\ &= \arg \min_{x \in \mathcal{X}} \sum_i f_i(x_{i*}) + \frac{\rho}{2} \sum_i \|R_i x_{i*} - r_i + \alpha_i^{(k)}\|_2^2 \\ &\quad + \frac{\rho}{2} \|x - z^{(k)} + \lambda^{(k)}\|_F^2. \end{aligned}$$

We rearrange the parentheses in Equation 2 to make the variables in each parenthesis mutually exclusive:

$$\begin{aligned} x^{(k+1)} &= \arg \min_{x \in \mathcal{X}} \sum_i \left(f_i(x_{i*}) + \frac{\rho}{2} \|R_i x_{i*} - r_i + \alpha_i^{(k)}\|_2^2 \right. \\ &\quad \left. + \frac{\rho}{2} \|x_{i*} - z_{i*}^{(k)} + \lambda_{i*}^{(k)}\|_2^2 \right). \end{aligned}$$

With the variable in each parenthesis mutually exclusive, we decompose to optimize per-resource allocation x_{i*} individually:

$$\begin{aligned} x_{i*}^{(k+1)} &= \arg \min_{x_{i*} \in \mathcal{X}_{i*}} \left(f_i(x_{i*}) + \frac{\rho}{2} \|R_i x_{i*} - r_i + \alpha_i^{(k)}\|_2^2 \right. \\ &\quad \left. + \frac{\rho}{2} \|x_{i*} - z_{i*}^{(k)} + \lambda_{i*}^{(k)}\|_2^2 \right). \end{aligned}$$

We follow a similar decomposing procedure for demand-constrained optimization on z :

$$\begin{aligned} z^{(k+1)} &= \arg \min_z \mathcal{L}_p(x^{(k+1)}, z, \alpha^{(k)}, \beta^{(k)}, \lambda^{(k)}) \quad (8) \\ &= \arg \min_z \sum_j g_j(z_{*j}) + \frac{\rho}{2} \sum_j \|D_j z_{*j} - d_j + \beta_j^{(k)}\|_2^2 \\ &\quad + \frac{\rho}{2} \|x^{(k+1)} - z + \lambda^{(k)}\|_F^2 \\ &= \arg \min_z \sum_j \left(g_j(z_{*j}) + \frac{\rho}{2} \|D_j z_{*j} - d_j + \beta_j^{(k)}\|_2^2 \right. \\ &\quad \left. + \frac{\rho}{2} \|x_{*j}^{(k+1)} - z_{*j} + \lambda_{*j}^{(k)}\|_2^2 \right). \end{aligned}$$

The optimization of z can now be decomposed into optimization on per-demand allocation z_{*j} :

$$\begin{aligned} z_{*j}^{(k+1)} &= \arg \min_{z_{*j}} \left(g_j(z_{*j}) + \frac{\rho}{2} \|D_j z_{*j} - d_j + \beta_j^{(k)}\|_2^2 \right. \\ &\quad \left. + \frac{\rho}{2} \|x_{*j}^{(k+1)} - z_{*j} + \lambda_{*j}^{(k)}\|_2^2 \right). \end{aligned}$$